Analysis of MTHFR, CBS, Glutathione, Taurine, and Hydrogen Sulfide Levels in Retinas of Hyperhomocysteinemic Mice

Xuezhi Cui,[1,2] Soumya Navneet,[1,2] Jing Wang,[1,2] Penny Roon,[1] Wei Chen,[3] Ming Xian,[3] and Sylvia B. Smith[1,2,4]

[1]Department of Cellular Biology and Anatomy, The Medical College of Georgia at Augusta University, Augusta, Georgia, United States
[2]The James and Jean Culver Vision Discovery Institute, Augusta University, Augusta, Georgia, United States
[3]Department of Chemistry, Washington State University, Pullman, Washington, United States
[4]Department of Ophthalmology, Augusta University, Augusta, Georgia, United States

Correspondence: Sylvia B. Smith, Department of Cellular Biology and Anatomy, Medical College of Georgia, Augusta University, Augusta, GA 30912-2000, USA; sbsmith@augusta.edu.

Submitted: December 8, 2016
Accepted: March 2, 2017

Citation: Cui X, Navneet S, Wang J, et al. Analysis of MTHFR, CBS, glutathione, taurine, and hydrogen sulfide levels in retinas of hyperhomocysteinemic mice. *Invest Ophthalmol Vis Sci*. 2017;58:1954–1963. DOI: 10.1167/iovs.16-21247

Purpose. Hyperhomocysteinemia (Hhcy) is implicated in certain retinal neurovascular diseases, although whether it is causative remains uncertain. In isolated ganglion cells (GCs), mild Hhcy induces profound death, whereas retinal phenotypes in Hhcy mice caused by mutations in remethylation (methylene tetrahydrofolatereductase [*Mthfr*$^{+/-}$]) or transsulfuration pathways (cystathionine β-synthase [*Cbs*$^{+/-}$]) demonstrate mild GC loss and mild vasculopathy. The current work investigated compensation in vivo of one pathway for the other, and, because the transsulfuration pathway yields cysteine necessary for formation of glutathione (GSH), taurine, and hydrogen sulfide (H_2S), they were analyzed also.

Methods. Retinas isolated from wild-type (WT), *Mthfr*$^{+/-}$, and *Cbs*$^{+/-}$ mice (12 and 22 weeks) were analyzed for methylene tetrahydrofolate reductase (MTHFR), cystathionine-β-synthase (CBS), and cystathionase (CTH) RNA/protein levels. Retinas were evaluated for levels of reduced:oxidized GSH (GSH:GSSG), Slc7a11 (xCT), taurine, taurine transporter (TAUT), and H_2S.

Results. Aside from decreased CBS RNA/protein levels in *Cbs*$^{+/-}$ retinas, there were minimal alterations in remethylation/transsulfuration pathways in the two mutant mice strains. Glutathione and taurine levels in *Mthfr*$^{+/-}$ and *Cbs*$^{+/-}$ retinas were similar to WT, which may be due to robust levels of xCT and TAUT in mutant retinas. Interestingly, levels of H_2S were markedly increased in retinas of *Mthfr*$^{+/-}$ and *Cbs*$^{+/-}$ mice compared with WT.

Conclusions. Ganglion cell loss and vasculopathy observed in *Mthfr*$^{+/-}$ and *Cbs*$^{+/-}$ mouse retinas may be milder than expected, not because of compensatory increases of enzymes in remethylation/transsulfuration pathways, but because downstream transsulfuration pathway products GSH, taurine, and H_2S are maintained at robust levels. Elevation of H_2S is particularly intriguing owing to neuroprotective properties reported for this gasotransmitter.

Keywords: remethylation pathway, transsulfuration pathway, retina, ganglion cell, homocysteine, one carbon metabolism

Homocysteine (Hcy) is a sulfur-containing nonproteinogenic amino acid, which sits at the intersection of the remethylation and transsulfuration metabolic pathways important for synthesis of methionine (Fig. 1). When the diet is replete with methionine, Hcy is catabolized to cystathionine by cystathionine-β-synthase (CBS) via the transsulfuration pathway. Cystathionine is converted to cysteine via cystathionase (CTH), also known as cystathionine γ-lyase (CSE). Cysteine is used in synthesis of downstream products such as glutathione (GSH), taurine, and hydrogen sulfide (H_2S). When the diet is deficient in methionine, Hcy is remethylated back to methionine via the remethylation pathway involving the enzymes methylene tetrahydrofolate reductase (MTHFR) and methionine synthase. The remethylation pathway requires folate and cobalamin (vitamin B_{12}) as cofactors. Perturbation in these pathways can lead to elevated plasma Hcy levels. Homozygous mutations in *Cbs* and *Mthfr* lead to homocystinuria characterized by exceedingly high levels of plasma Hcy, severe mental and skeletal abnormalities, premature thromboembolism, and lens dislocation.[1] Heterozygous mutations in these enzymes or nutritional deficiency of cofactors lead to moderate increase in plasma Hcy known as hyperhomocysteinemia (Hhcy).[2]

Hyperhomocysteinemia, an independent risk factor for cardiovascular diseases,[3] is implicated in certain neurodegenerative diseases.[4] Given that retina is a neurovascular tissue, there has been interest in the role of excess Hcy in retinal disease.[5] Some studies suggest that Hhcy plays a role in AMD,[6,7] diabetic retinopathy,[8–10] and retinal vein occlusion[11]; however, the mechanisms are not certain. Earlier studies suggested a link between Hhcy and glaucoma,[12,13] although recent reports raise doubt about this association.[14–20]

It is feasible to study effects of severely elevated Hhcy on retina using mice with global knockout of the *Cbs* or *Mthfr* genes.[21,22] It is perhaps more relevant to the general population to understand the effects of milder Hhcy on retina because of its greater prevalence. To understand the effects of chronic, but

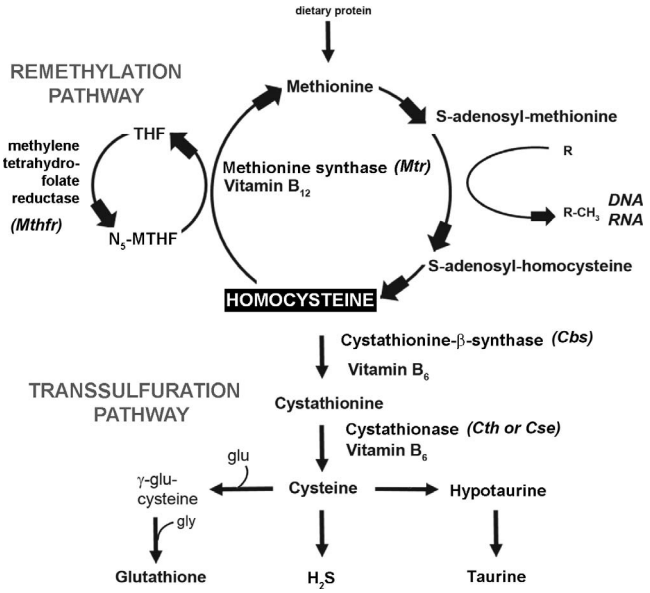

Figure 1. Homocysteine metabolic pathway. Homocysteine sits at the intersection of the remethylation and transsulfuration pathways. In the remethylation pathway, THF is converted to N_5,N_{10}-methylenetetrahydrofolate and then to MTHF by methylenetetrahydrofolate reductase (encoded by the gene *Mthfr*). The methyl group is donated to Hcy and in the presence of methionine synthase (encoded by *Mtr*), and B_{12} is converted to methionine. Methionine is used in many methyl transfer reactions. When the diet is replete with methionine, Hcy is converted, via the transsulfuration pathway, to cystathionine by cystathionine-β-synthase (encoded by *Cbs*) and then converted to cysteine via the action of cystathionase (encoded by *Cth,* also abbreviated *Cse*) in the presence of B_6. Cysteine is converted to several beneficial downstream products, some of which are essential for retinal function (glutathione and taurine). This current work investigated at the RNA and protein levels various aspects of this pathway in mice heterozygous for *Mthfr* and *Cbs*, which have mild Hhcy. Figure adapted with permission from Markand S, Saul A, Roon P, et al. Retinal ganglion cell loss and mild vasculopathy in methylene tetrahydrofolate reductase (Mthfr)-deficient mice: a model of mild hyperhomocysteinemia. *Invest Ophthalmol Vis Sci*. 2015;56:2684–2695.

milder elevation of Hcy on retina structure and function, our laboratory characterized the retinal phenotype in CBS- and MTHFR-deficient mice. *Cbs*$^{+/-}$ mice have an approximate 2-fold increase in retinal Hcy. The retinal morphology is comparable to that of age-matched wild-type (WT) mice initially, but by 15 to 30 weeks, morphologic changes are observed, including loss of cells in the ganglion cell (GC) layer and decreased thickness of inner plexiform and nuclear layers.[21] Functional studies reveal a gradual decrease in electroretinogram (ERG) amplitudes by 10 weeks of age.[23] There is mild vasculopathy observed in *Cbs*$^{+/-}$ mice that worsens significantly with age and includes neovascularization, vessel tortuosity, vascular leakage, and areas of ischemia/hypoxia.[24] Retinas of these mice demonstrate elevated glial fibrillary acidic protein (GFAP) consistent with retinal gliosis.[24] *Mthfr*$^{+/-}$ mice also have a slight elevation (approximately 2-fold) of retinal Hcy. The mice have no significant differences in scotopic or photopic a- or b-wave amplitudes of the ERG; however, they demonstrate a decrease in the positive scotopic threshold responses (STRs) at 12 weeks, which becomes more pronounced at 24 weeks, consistent with modest attenuation of ganglion cell function.[25] Fluorescein angiographic analysis of *Mthfr*$^{+/-}$ mutants showed focal leakage and vascular tortuosity by 24 weeks. Optical coherence tomography (OCT) imaging of *Mthfr*$^{+/-}$ revealed a statistically significant decrease in the nerve fiber layer (NFL) thickness at 24 weeks. The loss of GCs and decreased NFL thickness is not associated with increased intraocular pressure.[25]

The data from studies of *Cbs*$^{+/-}$ and *Mthfr*$^{+/-}$ mice support the idea that the mild retinal neurovasculopathy is due to chronic exposure to slightly elevated Hcy levels. It is important to note, however, that the retinopathy develops over many weeks and does not overwhelm the visual system to the point of blindness. This observation contrasts with data obtained in isolated primary GCs harvested from WT mice exposed to Hcy. Even fairly low level exposure to Hcy (50 μM for 18 hours) can induce death in ~50% of cells.[26] Clearly, the intact retinal milieu has the capacity to withstand exposure to mild Hhcy. We do not know whether in the in vivo models there is any compensatory effect, such that *Cbs* expression is altered in *Mthfr* mutants or vice versa. We addressed this in the current study by evaluating CBS and MTHFR at the RNA and protein level in retinas of *Cbs*$^{+/-}$ and *Mthfr*$^{+/-}$ mice. In addition, we had not previously assessed levels of potentially beneficial downstream products of the transsulfuration pathway (GSH, taurine, and H_2S; Fig. 1) in retinas of these mutant mice, but do so in the current study. Glutathione is an abundant antioxidant in the retina that affords protection to the highly oxidative retinal environment. A naturally occurring tripeptide formed of glutamate, glycine, and cysteine, GSH acts as a reductant of peroxides.[27] Taurine is the most abundant amino acid in retina and is essential for normal retinal architecture and function.[28] Hydrogen sulfide is a gasotransmitter that has neuroprotective properties.[29] The current study analyzed levels of GSH, taurine, and H_2S in retinas of both mutant mouse strains. We found that GSH and taurine levels were similar between the mutant mouse strains and WT. Most interesting was the observation that levels of H_2S were actually elevated in retinas of both mutant mouse strains, which may account for the milder-than-expected phenotypes in the mice. The elevated H_2S also raises intriguing questions about the role of Hcy in regulating levels of this gasotransmitter. For the current work, two ages were selected for analysis (12 and 22 weeks) because they reflect time points in which only modest GC loss is observed, mild retinal function alteration is detected, and vasculopathy is modest in both mutant strains.

Methods

Animals

Eighty-two mice were used in the study (Table 1). Breeding pairs of *Mthfr*$^{+/-}$ mice (Rozen Lab, McGill University, Montreal, Canada) and *Cbs*$^{+/-}$ mice (B6.129P2-Cbs^{tm1Unc}/J; Jackson Laboratories, Bar Harbor, ME, USA) were used to establish colonies of these strains. Confirmation of the genotype was performed as described.[21,25] Briefly, DNA was prepared from a small tissue sample from the mouse ear by NaOH (HotSHOT) extraction followed by PCR. Primers used for genotyping *Mthfr* were as follows: mmrEx3S (5′-GAA GCA GAG GGA AGG AGG CTT CAG-3′); nEOs5 (5′-AGC CTG AAG AAC GAG ATC AGC AGC-3′); and mIN3A1 (5′-GAC TAG CTG GCT ATC CTC TCA TCC-3′). Polymerase chain reaction yielded a single band of ~145 bp for WT mice and two bands for the heterozygous mice (~216 bp; Fig. 2A). Primers used for genotyping *Cbs* were as follows: P10 (5′-GAA GTG GAG CTA TCA GAG CA-3′); Pneo (5′-GAG GTC GAC GGT ATC GAT A-3′); and P13 (5′-CGG ATG ACC TGC ATT CAT CT-3′). The PCR yielded a single band of ~510 bp for WT mice and two bands for the heterozygous mice (~450 bp; Fig. 2B). Mice were also screened for the Crb1$^{rd8/rd8}$ mutation and were negative. The Crb1$^{rd8/rd8}$ mutation, which causes focal disruption of the retina, has

Table 1. Animals Used in This Study

Mouse Genotype	*n*	Age, wk
qRt-PCR analysis to examine Mthfr, Cbs, Cth, and Slc7a11(xCT) gene expression in the mouse retina		
Mthfr$^{+/+}$, Cbs$^{+/+}$ (wild-type)	3	12
Mthfr$^{+/-}$ (heterozygous)	3	12
Cbs$^{+/-}$ (heterozygous)	3	12
Mthfr$^{+/+}$, Cbs$^{+/+}$ (wild-type)	3	22
Mthfr$^{+/-}$ (heterozygous)	3	22
Cbs$^{+/-}$ (heterozygous)	3	22
Western blot analysis to examine MTHFR, CBS, CTH, xCT, TAUT, and 3MST protein expression in the mouse retina		
Mthfr$^{+/+}$, Cbs$^{+/+}$ (wild-type)	5	12
Mthfr$^{+/-}$ (heterozygous)	5	12
Cbs$^{+/-}$ (heterozygous)	5	12
Mthfr$^{+/+}$, Cbs$^{+/+}$ (wild-type)	5	22
Mthfr$^{+/-}$ (heterozygous)	5	22
Cbs$^{+/-}$ (heterozygous)	5	22
H_2S and reduced GSH detection in the mouse retina		
Mthfr$^{+/+}$, Cbs$^{+/+}$ (wild-type)	4	12
Mthfr$^{+/-}$ (heterozygous)	4	12
Cbs$^{+/-}$ (heterozygous)	4	12
Mthfr$^{+/+}$, Cbs$^{+/+}$ (wild-type)	4	22
Mthfr$^{+/-}$ (heterozygous)	4	22
Cbs$^{+/-}$ (heterozygous)	4	22
Amino acid profile for taurine levels in the mouse retina		
Mthfr$^{+/+}$, Cbs$^{+/+}$ (wild-type)	2	12
Mthfr$^{+/-}$ (heterozygous)	1	12
Cbs$^{+/-}$ (heterozygous)	2	12
Mthfr$^{+/+}$, Cbs$^{+/+}$ (wild-type)	2	22
Mthfr$^{+/-}$ (heterozygous)	1	22
Cbs$^{+/-}$ (heterozygous)	2	22

been reported in various mouse strain stocks, and it is important to exclude these mutant alleles before studying new retinal models.[30] Breeder C57BL/6J (WT) mice were from Jackson Labs. Mice were fed Teklad Irradiated Rodent Diet 8904 for breeding or Diet 2918 for maintenance (Teklad, Madison, WI, USA). Animals were subjected to a standard 12-hour light:12-hour dark cycle. Maintenance and treatment of animals adhered to institutional guidelines for humane treatment of animals and to the ARVO statement for Use of Animals in Ophthalmic and Vision Research.

Quantitative RT-PCR Analysis of Gene Expression

Total RNA was isolated from neural retina using TRIzol (Invitrogen, Carlsbad, CA, USA). Two micrograms RNA was converted to cDNA using the iScript synthesis kit (Bio-Rad Laboratories, Hercules, CA, USA). The primers used to detect *Mthfr, Cbs, Cth*, and *Slc7a11* (*xCT*) were obtained from Integrated DNA Technologies (Redwood City, CA, USA) (Table 2). Glyceraldehyde 3-phosphate dehydrogenase (*GAPDH*) served as an internal control. Quantitative RT-PCR was performed using the SsoAdvanced SYBR Green Supermix from Bio-Rad (Hercules, CA, USA) and the Bio-Rad CFX96-Real Time System Thermal Cycler. Polymerase chain reaction was performed at 95°C for 30 seconds, 63°C for 30 seconds, and 72°C for 45 seconds; melt curve analysis confirmed the purity of the end products. Resulting C_Q values were normalized to *Gapdh* and analyzed using the comparative C_Q method[31,32] to obtain fold-changes in gene expression. The analysis was performed in triplicate.

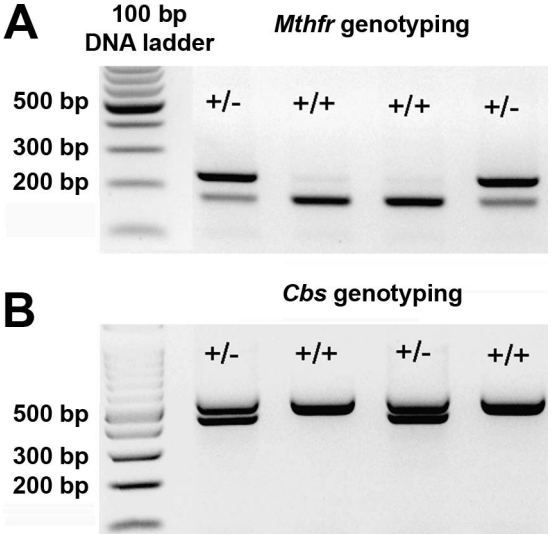

Figure 2. Genotype assessment of *Mthfr* and *Cbs* in mouse retina. Retinas were isolated for PCR analysis to determine genotyping as described in the text. (**A**) *Mthfr* genotyping data for four representative offspring; mice expressing only the 145-bp product have both copies of *Mthfr* gene and are designated wild-type (+/+); mice expressing both the 216- and the 145-bp products have one copy of *Mthfr* (heterozygous, +/–). (**B**) *Cbs* genotyping data for four representative offspring; mice expressing only the 510-bp product have both copies of *Cbs* gene and are wild-type (+/+); mice expressing both the 510- and 450-bp products have one copy of *Cbs* (heterozygous, +/–). The 100-bp DNA ladder was used as the reference.

Immunodetection of Proteins in Mouse Retina

Protein was extracted from neural retinas of WT, *Mthfr*$^{+/-}$, and *Cbs*$^{+/-}$ mice per our method.[21,24,31,32] Forty to 100 µg protein was subjected to SDSPAGE at 100 V and transferred to nitrocellulose membranes at 90 V for 1.5 hours. Membranes were blocked in 5% milk in TBST (1 hour at room temperature), followed by incubation with primary antibodies: goat anti-MTHFR (Abcam, Cambridge, MA, USA; 1:500), rabbit anti-CBS (Cell Signaling, Danvers, MA, USA; 1:250), rabbit anti-CTH (Thermo-Fisher Scientific, Waltham, MA, USA; 1:500), rabbit anti-3MST (Aviva Systems Biology, San Diego, CA, USA; 1:500), rabbit anti-xCT[33] (1:800), and rabbit anti–taurine transporter (TAUT) (Alomone Labs, Jerusalem, Israel; 1:200) in 5% milk in TBST buffer at 4°C overnight. Membranes were washed three times for 5 minutes in TBST and incubated with horseradish peroxidase–conjugated goat anti-rabbit IgG antibody (Santa Cruz Biotechnology, Santa Cruz, CA, USA; 1:2000) for 1 hour at room temperature. The ECL Western blot detection system (Thermo Scientific) was used to visualize protein bands. Membranes were reprobed with GAPDH (Millipore, Temecula, CA, USA), which served as the loading control. All immunoblot images are representative of three or more independent experiments. The bands from Western blotting were quantified using Image J 1.48v software (http://imagej.nih.gov/ ij/; National Institutes of Health, Bethesda, MD, USA).

Assessment of GSH, Taurine, and H_2S Levels in Mouse Retina

Retinas were harvested from euthanized WT, *Mthfr*$^{+/-}$, and *Cbs*$^{+/-}$ mice by proptosing the eye using Dumont #5 forceps and slitting the cornea using a #15 scalpel blade. After the lens was gently ejected, the retina was lifted way from the eyecup using the forceps. Retinas were homogenized in ice-cold PBS

Table 2. PCR Primers Used for Gene Expression Studies

Gene	NCBI Accession Number	Primer Sequence	
		Forward	Reverse
Gapdh	NM_008084	5′-AGGTCGGTGTGAACGGATTTG-3′	5′-TGTAGACCATGTAGTTGAGGTCA-3′
Mthfr	NM_010840	5′-ACAGGCCATCTGCACAGAGCCAA-3′	5′-CAGTTTTACAAGCTGCCGAAGGGA-3′
Cbs	NM_144855	5′-CCAGGCACCTGTGGTCAAC-3′	5′-GGTCTCGTGATTGGATCTGCT-3′
Cth	NM_145953	5′-TTCCTGCCTAGTTTCCAGCAT-3′	5′-GGAAGTCCTGCTTAAATGTGGTG-3′
Slc7a11 (xCT)	NM_011990	5′-GGCACCGTCATCGGATCAG-3′	5′-CTCCACAGGCAGACCAGAAAA-3′

and centrifuged at 10,000*g* for 10 minutes at 4°C; supernatant was used for GSH and H_2S detection. Protein concentration was determined using the Pierce BCA protein assay kit (Thermo-Fisher Scientific).

To estimate levels of GSH, cellular GSH levels per protein and glutathione redox state (GSH/GSSG) were determined using the Glutathione Detection Kit (ADI-900-160; Enzo Life Sciences, Farmingdale, NY, USA) according to the manufacturer's instructions. The supernatant was treated with metaphosphoric acid (MPA, final concentration 5%; Sigma-Aldrich Corp., St. Louis, MO, USA) for 5 minutes. A diluted known volume of MPA extract was treated without (for total GSH) or with 4-vinylpyridine (Sigma-Aldrich Corp.) (only for GSSG analysis), and appropriate GSSG standards were treated similarly to prepare a standard curve. After appropriate volumes of freshly prepared reaction mix (glutathione reductase with reaction mix buffer) were added, a kinetic GSH-reductase recycling assay was performed following the manufacturer's instructions using a Synergy Multi-Mode Reader (BioTek, Winooski, VT, USA) set at 405 nm and read at 1-minute intervals over 10 minutes.

Taurine levels were determined in isolated retina by adding 10% sulfosalicylic acid (SSA) (1 mg retina [wt]:200 μL 10% SSA [vol]) to the sample for deproteinization by sonication. Two hundred microliters was removed, centrifuged at 3000*g* for 15 minutes, and dissolved in PBS for protein determination. The remaining mixture was centrifuged at 10,000*g* for 25 minutes; supernatant was filtered through a 0.45-mm syringe–driven polytetrafluoroethylene (PTFE) filter. The pH was adjusted to 2.2 by adding 0.3 N LiOH to the supernatant in a ratio of 4:1 and loaded to a Biochrom 30 amino acid analyzer (Biochrom US, Holliston, MA, USA). The analysis was performed by the Amino Acid Laboratory, School of Veterinary Medicine at University of California Davis.

To detect H_2S, we followed the method of Zhang et al.[34] Briefly, 20 μL retinal supernatant (prepared as described above) was mixed with 69 μL PBS and distilled H_2O (10, 9.6, 8.8, and 8.4 μL, respectively). Thereafter, 0, 0.4, 0.8, 1.2, and 1.6 μL Na_2S stock solution (100 μM) was spiked into samples as an internal standard (X, X + 0.4, X + 0.8, X + 1.2, X + 1.6 μM), followed by the addition of 1 μL 1 mM WSP-5 probe[35] (final concentration 10 μM and 5 mM) and cetrimonium bromide (CTAB) (final concentration 100 μM). The WSP-5 probe has been fully characterized and is selectively sensitive to H_2S in the low nanomolar range.[35] Following a 20-minute incubation, fluorescence was measured using the Synergy 2 plate reader set at excitation:emission of 485:525 nm. The zero point was obtained by addition of 1 μL 100 mM $ZnCl_2$ to trap H_2S in the samples. The sulphide concentration per sample was calculated using a calibration curve of Na_2S, and results are expressed as μmol/g protein.

Statistical Analysis

Two-way ANOVA was used to test for significant differences between the three mouse groups (WT, *Mthfr*$^{+/-}$, and *Cbs*$^{+/-}$) at the two ages (12 and 22 weeks) studied. Tukey's paired comparison test was the post hoc statistical test. Statistical analysis used the GraphPad Prism software (version 6; GraphPad Software, Inc., La Jolla, CA, USA). $P < 0.05$ was considered significant.

Results

Assessment of MTHFR and CBS in *Mthfr*$^{+/-}$ and *Cbs*$^{+/-}$ Retinas

We evaluated *Mthfr, Cbs,* and *Cth* RNA levels and MTHFR, CBS, and CTH protein levels in retinas of *Mthfr*$^{+/-}$ mice at 12 and 22 weeks. We used both retinas from a single mouse for RNA expression studies with at least three repetitions of the analysis. Similarly, we used both retinas from a single mouse to evaluate protein levels, again with at least three repetitions. Retinal expression of *Mthfr* in *Mthfr*$^{+/-}$ mice was noticeably decreased by 22 weeks (Fig. 3A); protein levels of MTHFR were only mildly (and not significantly) altered at this age (Fig. 3B). Quantitative data from three separate immunoblotting experiments are presented in Figure 3C. Interestingly, expression of *Cbs* increased significantly in *Mthfr*$^{+/-}$ mice at 12 weeks, although it decreased significantly by 22 weeks (Fig. 3D). Protein levels of CBS showed a similar trend in levels, but did not reach statistical significance (Figs. 3E, 3F). Evaluation of *Cth* in *Mthfr*$^{+/-}$ mice showed a significant increase in expression at 12 weeks but no difference at 22 weeks (Fig. 3G). The CTH protein levels evaluated in WT and *Mthfr*$^{+/-}$ mice showed no difference at either 12 or 22 weeks (Figs. 3H, 3I). The data suggest that, in the *Mthfr*$^{+/-}$ mouse retina, there is a detectable difference in expression of *Cbs* as well as *Mthfr*, but no significant change in levels of these proteins in mice hyperhomocysteinemic due to *Mthfr* mutation.

We next evaluated RNA and protein levels in retinas of *Cbs*$^{+/-}$ mice at 12 and 22 weeks. Following the same sequence as described above, we first examined expression of *Mthfr* in *Cbs*$^{+/-}$ mice: there was no change at 12 weeks; there was, however, a significant decrease in *Mthfr* expression at 22 weeks (Fig. 4A). Analysis of MTHFR protein levels in three independent samples showed a trend toward decreasing protein levels at 22 weeks in *Cbs*$^{+/-}$ mutant mice compared with WT (Figs. 4B, 4C); however, the data did not reach statistical significance. Examination of *Cbs* expression in *Cbs*$^{+/-}$ retinas revealed significant decreases at 12 and 22 weeks compared with WT (Fig. 4D). Levels of the CBS protein were slightly lower in retinas of *Cbs*$^{+/-}$ mice at 12 weeks compared with WT but were markedly decreased by 22 weeks in the mutant compared with age-matched WT mice (Figs. 4E, 4F). Regarding RNA and protein levels of CTH, there were no differences between *Cbs*$^{+/-}$ and WT at either 12 or 22 weeks (Figs. 4G–I).

Taken collectively, data shown in Figures 3 and 4 suggest that there is not a compensatory increase in levels of key enzymes of the transsulfuration pathway (CBS, CTH) in *Mthfr*$^{+/-}$ mice nor a compensatory increase in levels of

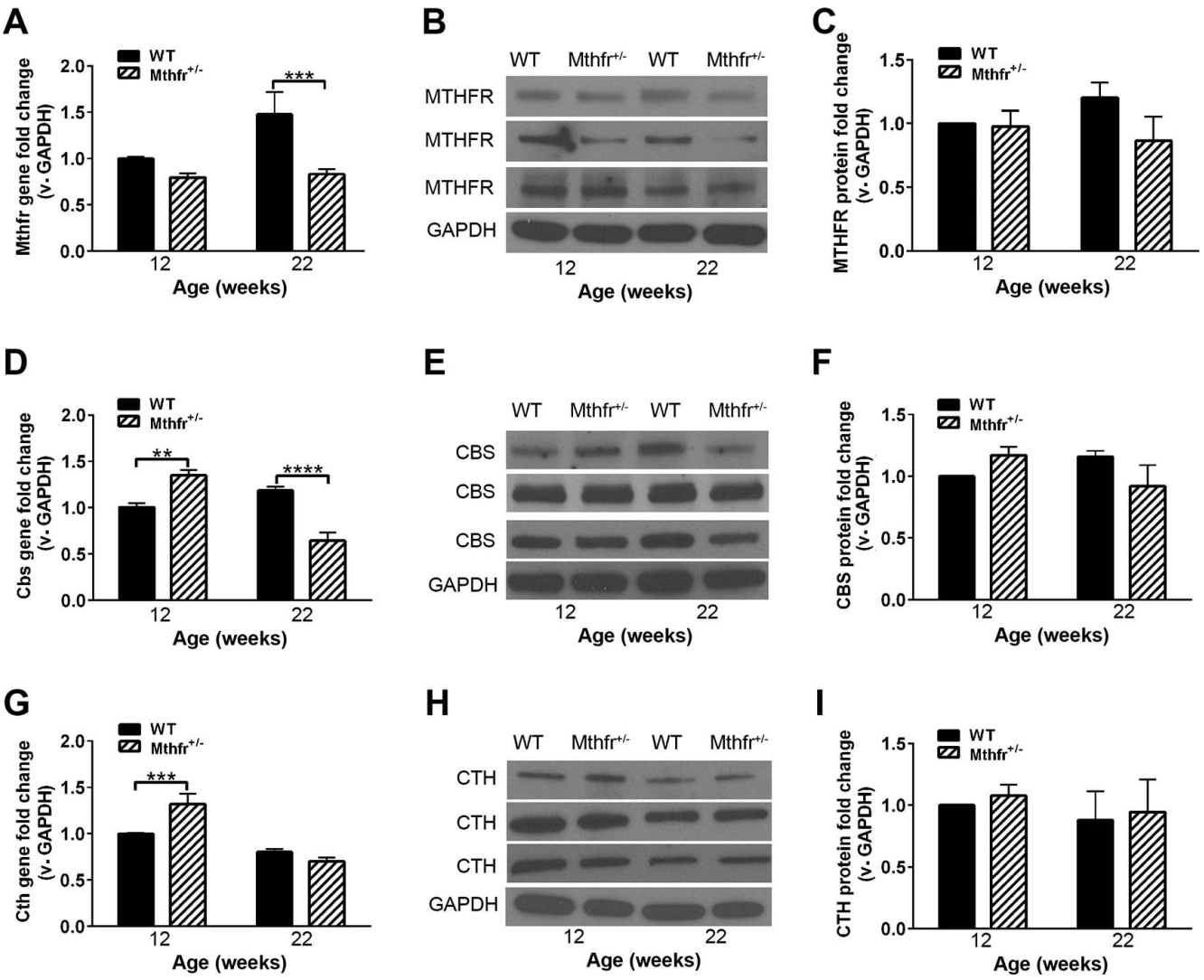

Figure 3. Analysis of genes and proteins in *Mthfr*$^{+/-}$ mice. Retinas were harvested from 12- and 22-week WT and *Mthfr*$^{+/-}$ mice and were used for isolation of RNA and protein. Quantitative real-time RT-PCR analysis of (**A**) *Mthfr*, (**D**) *Cbs*, and (**G**) *Cth* in 12- and 22-week WT and *Mthfr*$^{+/-}$ mice. *Error bars* represent the mean ± SEM from three separate experiments ($n = 3$). Representative immunoblotting data for three experiments detecting levels of (**B**) MTHFR, (**E**) CBS, and (**H**) CTH in WT and *Mthfr*$^{+/-}$ mice. GAPDH was used as the internal control. In this figure, the GAPDH bands shown relate to the *upper panel* for each experiment. GAPDH was evaluated for each separate experiment; the quantification of band densities is shown as a ratio of protein: GAPDH for (**C**) MTHFR, (**F**) CBS, and (**I**) CTH in WT and *Mthfr*$^{+/-}$ mice. *Error bars* represent the mean ± SEM from three separate experiments ($n = 3$). $^{**}P < 0.01$, $^{***}P < 0.001$, $^{****}P < 0.0001$.

MTHFR in retinas of *Cbs*$^{+/-}$ mice. There is a substantial decrease in CBS protein levels in retinas of the *Cbs* heterozygous mice, whereas levels of MTHFR protein in the *Mthfr*$^{+/-}$ mouse retina are similar to WT. Protein levels of CTH were not altered in either mutant strain.

Given that there was a significant decrease in CBS protein level in *Cbs*$^{+/-}$ mouse retinas, we were interested in determining levels of downstream products in the transsulfuration pathway secondary to synthesis of cysteine, including GSH, taurine, and H_2S.

Assessment of GSH, Taurine, and H_2S in *Mthfr*$^{+/-}$ and *Cbs*$^{+/-}$ Retinas

Reduced GSH is one of the most important scavengers of reactive oxygen species (ROS), and its ratio with GSSG may be used as a marker of oxidative stress. We used a commercially available kit to analyze levels of GSH and determine the GSH/GSSG ratio in retinal samples. Our data show that GSH levels in retinas of *Mthfr*$^{+/-}$ and *Cbs*$^{+/-}$ retinas did not differ significantly from WT retinas (Fig. 5A). Similarly, the ratio of reduced to oxidized glutathione was similar between WT and mutant retinas (Fig. 5B). Glutathione is a tripeptide formed by linkage of glutamate-cysteine-glycine. Cysteine is the rate-limiting substrate for de novo GSH synthesis. Although the transulfuration pathway is a source of cysteine, there are other mechanisms by which cells can acquire cysteine for GSH synthesis including the Na^+-independent cystine-glutamate exchanger, system x_c^-. Whereas CBS is decreased in *Cbs*$^{+/-}$ mice (Figs. 4D, 4E), cysteine could be available to retinas of mutant mice via this exchanger, which is expressed in multiple retinal cell types.[36] System x_c^- is composed of two subunits: the transport specific xCT subunit and the ubiquitous 4F2hc subunit.[37] Under physiologic conditions, system x_c^- transports cystine into cells coupled to efflux of glutamate out of cells. Once inside the cell, cystine is converted to cysteine and used in GSH synthesis. We examined xCT at the RNA and protein level in *Mthfr*$^{+/-}$ retinas (Figs. 5C–E) and *Cbs*$^{+/-}$ retinas (Figs.

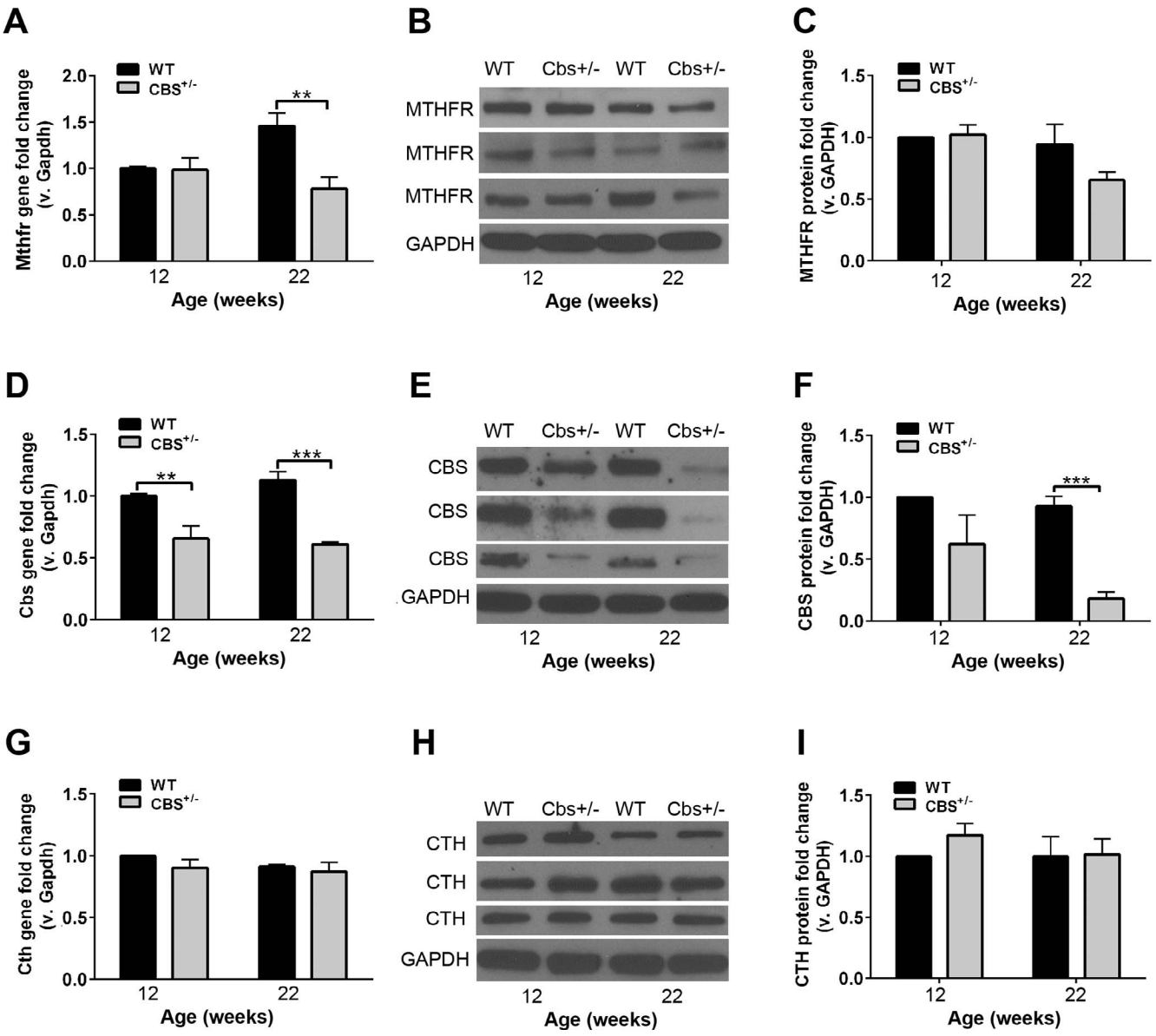

Figure 4. Analysis of genes and proteins in *Cbs*$^{+/-}$ mice. Retinas were harvested from 12- and 22-week WT and *Cbs*$^{+/-}$ mice and were used for isolation of RNA and protein. Quantitative real-time RT-PCR analysis of (**A**) *Mthfr*, (**D**) *Cbs*, and (**G**) *Cth* in 12- and 22-wk WT and Cbs$^{+/-}$ mice. *Error bars* represent the mean ± SEM from three separate experiments ($n = 3$). Representative immunoblotting data for three experiments detecting levels of (**B**) MTHFR, (**E**) CBS, and (**H**) CTH in WT and *Cbs*$^{+/-}$ mice. GAPDH was used as the internal control. In this figure, the GAPDH bands shown relate to the *upper panel* for each experiment. GAPDH was evaluated for each separate experiment; the quantification of band densities is shown as a ratio of protein:GAPDH for (**C**) MTHFR, (**F**) CBS, and (**I**) CTH in WT and *Cbs*$^{+/-}$ mice. *Error bars* represent the mean ± SEM from three separate experiments ($n = 3$). $^{**}P < 0.01$, $^{***}P < 0.001$, $^{****}P < 0.0001$.

5F–H) and found that expression levels were similar to WT. Our data suggest that levels of GSH are maintained in the Hhcy retinas, due at least in part, to robust expression of system x_c^-, and are therefore not decreased by disruption of the transulfuration pathway.

We then evaluated the level of taurine in retinas of *Mthfr*$^{+/-}$ and *Cbs*$^{+/-}$ mice. Taurine is an enigmatic molecule. It is the most abundant amino acid in the retina, and it is essential for maintenance of photoreceptor cells, yet its physiologic role is unclear. Because taurine is downstream in the transulfuration pathway, we were interested in determining whether its normally high levels would be altered in retinas of mice with disruption of this pathway. Our analysis used retinal samples from mice at 12 and 22 weeks. The levels of taurine were quite high at 12 weeks in WT and the *Mthfr*$^{+/-}$ and *Cbs*$^{+/-}$ mice (~800 nmol/mg protein) and slightly less at 22 weeks (Fig. 6A). Two-way ANOVA showed no difference in taurine levels for either age or mouse group analyzed. It addition to its synthesis in the transsulfuration pathway, taurine can be supplied also to tissues via TAUT, which is present in a number of cells within the retina.[38] We examined the level of TAUT in WT and mutant mouse retinas at 12 and 22 weeks. In all cases, TAUT was detected abundantly, suggesting its active role in retinas of these mice (Fig. 6B). It appears that even though the transulfuration pathway is decreased in *Cbs*$^{+/-}$ mice, taurine levels and levels of TAUT are maintained in retinas of these mice and *Mthfr*$^{+/-}$ mice.

We next evaluated levels of H_2S in retinas of *Mthfr*$^{+/-}$ and *Cbs*$^{+/-}$ mice using a probe that is specific for this gasotransmitter.[35] The basis of detection is the dual nucleophilicity of

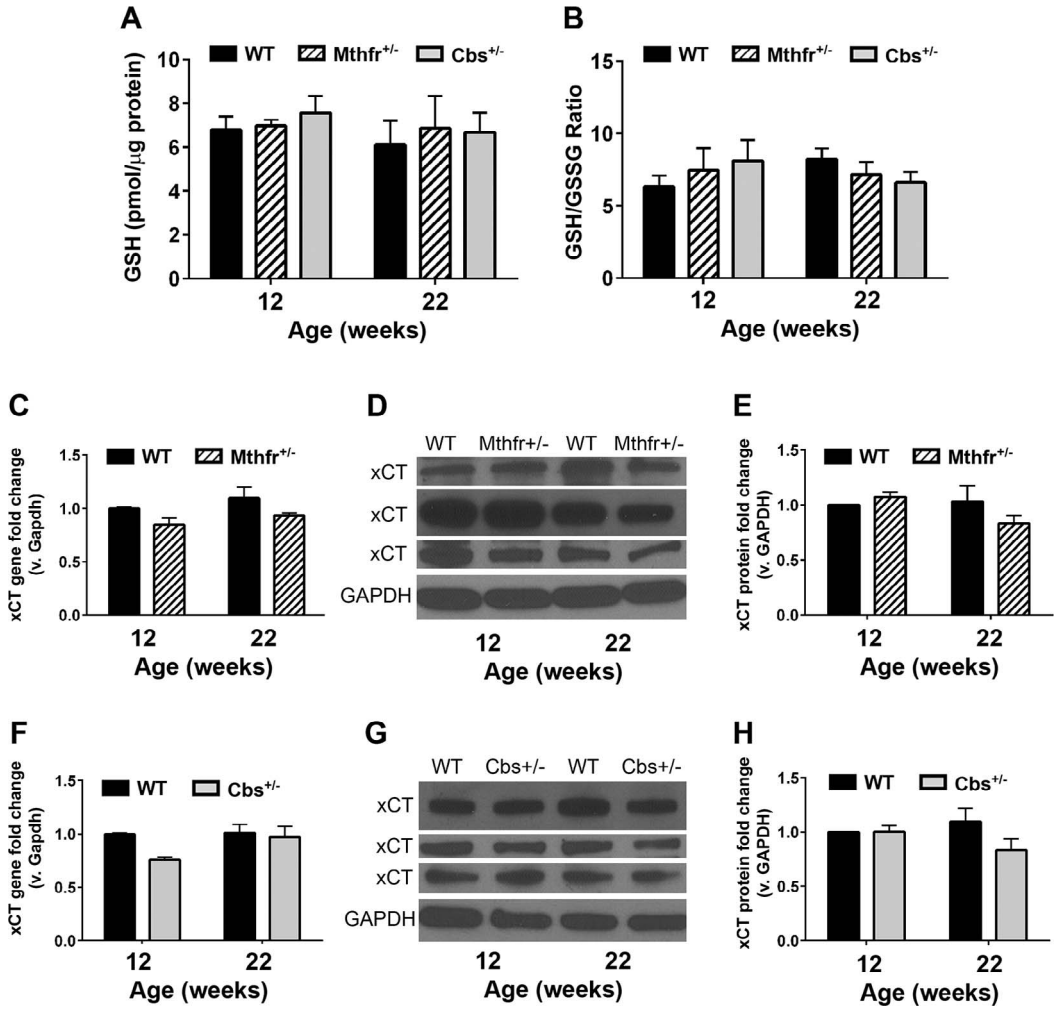

Figure 5. Detection of GSH and xCT (Slc7a11). Retinas were harvested from 12- and 22-wk WT, *Mthfr*$^{+/-}$, and *Cbs*$^{+/-}$ mice and were used to detect (**A**) reduced GSH (pmol/mg protein) and (**B**) glutathione redox ratio (GSH/GSSG) using a commercially available kit according to the manufacturer's instructions. There were no statistically significant differences between the groups. Each experiment was performed in triplicate. Additional retinas were harvested from WT, *Mthfr*$^{+/-}$, and *Cbs*$^{+/-}$ mice to evaluate expression of xCT. (**C**, **F**) Quantitative real-time RT-PCR analysis of *xCT* mRNA extracted from 12- and 22-wk WT, *Mthfr*$^{+/-}$, and *Cbs*$^{+/-}$ mice. Primers are provided in Table 2. There were no significant differences in gene expression. (**D**, **G**) Representative immunoblots to detect xCT in proteins extracted from 12- and 22-wk WT, *Mthfr*$^{+/-}$, and *Cbs*$^{+/-}$ mice. (**E**, **F**) Quantification of immunoblotting data. *Error bars* represent mean ± SEM from three separate experiments ($n = 3$). There were no significant differences in levels of xCT.

H_2S and a H_2S-mediated tandem nucleophilic substitution-cyclization reaction, which is used to release fluorophores and turn on fluorescence. The probe (WSP-5) shows high sensitivity and selectivity for H_2S over other reactive sulfur species (e.g., cysteine and GSH).[35] Interestingly, H_2S levels were elevated significantly in mutant retinas compared to WT (Fig. 7A). Hydrogen sulfide measured at 12 weeks in retinas of WT animals averaged ~1.35 μM/g protein, whereas age-

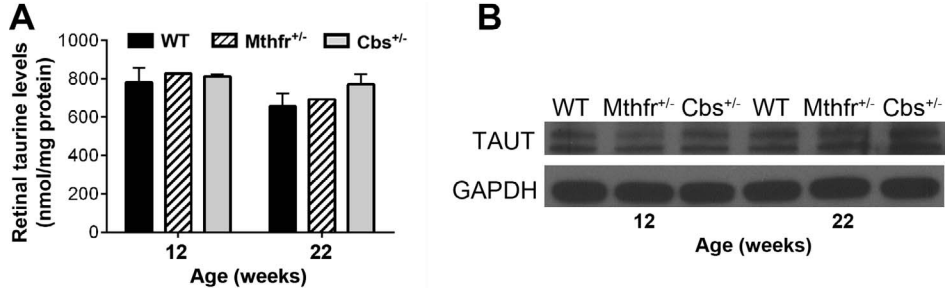

Figure 6. Analysis of retinal taurine levels and taurine transporter (TAUT). Retinas were harvested from 12- and 22-wk WT, *Mthfr*$^{+/-}$, and *Cbs*$^{+/-}$ mice and were used to detect taurine levels using an amino acid analyzer and levels of TAUT by immunoblotting. (**A**) Quantitative data of retinal taurine levels analyzed as described in the text. (**B**) Representative immunoblot showing detection of TAUT. GAPDH was used as the internal control. There were no statistically significant differences between the groups from triplicate experiments.

Figure 7. Analysis of H_2S and MST. Retinas were harvested from 12- and 22-wk WT, *Mthfr*$^{+/-}$, and *Cbs*$^{+/-}$ mice and were used to measure H_2S (sulphide concentration, µmol/g protein) using fluorescence probe WSP-5 as described. Data are mean ± SEM from three separate experiments ($n = 3$). $^{*}P < 0.05$, $^{**}P < 0.01$. (**B**) Additional retinas were harvested from 12- and 22-wk WT, *Mthfr*$^{+/-}$, and *Cbs*$^{+/-}$ mice and protein isolated; representative immunoblot shows detection of MST; GAPDH was the internal control. (**C**) Quantification of immunoblotting data. *Error bars* represent mean ± SEM from three separate experiments ($n = 3$). There were no significant differences in levels of MST.

matched *Mthfr*$^{+/-}$ and *Cbs*$^{+/-}$ retinas had H_2S levels that were 2-fold higher (~3.5 µM/g). Wild-type mice at 22 weeks had a slight increase in H_2S levels versus younger WT mice (~1.9 µM/g), but levels were still significantly less than the mutant mice (~3.3 µM/g). Hydrogen sulfide is predominantly formed from cysteine by the enzymes CBS or CTH.[29] Our data, shown in Figure 4, indicated that CBS was decreased significantly in *Cbs*$^{+/-}$ mutant retinas; thus, the elevation of H_2S was surprising in these mutants. The observation of elevated H_2S in the two hyperhomocysteinemic models presents an interesting conundrum as elevated H_2S can have cytoprotective and cytodisruptive effects as discussed below. Recent studies suggest that H_2S can be generated also by a third enzyme: 3-mercaptopyruvate sulfurtransferase (MST).[29] We examined levels of MST protein in retinas of *Mthfr*$^{+/-}$ and *Cbs*$^{+/-}$ mice, and representative immunoblotting data are shown (Fig. 7B). MST was detected in retinas as has been reported.[39] Quantification of five separate immunoblotting experiments showed a slight increase in MST in retinas of *Mthfr*$^{+/-}$ compared with WT and *Cbs*$^{+/-}$ mice at 12 weeks and a slight decrease in this protein in *Mthfr*$^{+/-}$ versus *Cbs*$^{+/-}$ and WT mice at 22 weeks (Fig. 7C); however, quantitative analysis revealed no statistically significant difference in MST protein levels between the three groups at either age.

Discussion

Elevated Hcy levels are implicated in retinal neurovascular diseases including central retinal vein occlusion (CRVO), pseudoexfoliation glaucoma, and diabetic retinopathy.[5] Controversy exists as to whether Hhcy is a biomarker or pathogenic in retinopathies. Efforts to resolve this controversy have used in vitro models and subsequently in vivo models. In vitro studies performed using GCs isolated from mouse retina showed marked vulnerability to micromolar concentrations of Hcy such that incubation of the cells 18 hours with 50 µM D,L-hcy thiolactone led to 50% cell death.[40] In vivo studies demonstrated profound GC loss and inner retinal disruption within 5 days of intravitreal injection of high dosage (200 µM) of D,L-hcy thiolactone.[41] Marked photoreceptor cell loss within 15 days and complete ablation of the outer nuclear layer within 90 days after hcy-thiolactone intravitreal injection (25 and 200 µM) was reported by Chang et al.[42]

Effects of more physiologically relevant concentrations of Hhcy can be studied using mice that harbor mutations of genes, such as *Cbs* and *Mthfr*, which cause Hhcy in the human population. We reported previously that the retinal phenotype is similar in mice with heterozygous mutations of either *Cbs*[21,23,24] or *Mthfr*.[25] For example, *Cbs*$^{+/-}$ and *Mthfr*$^{+/-}$ mice demonstrate loss of GCs yet little involvement of inner or outer nuclear retinal layers. Both mutant mice demonstrate electrophysiologic deficits that reflect compromised GC function, although intact photoreceptor-bipolar responses. There are alterations in the thickness in *Mthfr*$^{+/-}$ mice[25] and decreased mitochondrial size in the NFL in *Cbs*$^{+/-}$ mice.[43] Both mutant models have elevated glial acidic fibrillary protein (GFAP) levels, suggestive of active gliosis ongoing within the retina. Finally, the mutant mice show vascular changes, although the extent of the vasculopathy appears worse in *Cbs*$^{+/-}$[24] compared with *Mthfr*$^{+/-}$ mice.[25] The data suggest that chronic endogenous Hhcy is mildly deleterious to retinal neurons and vasculature. These observations in the mouse models are relevant to humans. For examples, higher serum Hcy levels and altered one-carbon metabolism have been reported in a subset of astronauts on the International Space Station who developed ophthalmic changes including altered NFL thickness, optic disc edema, globe flattening, choroidal folds, hyperopic shifts, and cotton wool spots.[44] There was no evidence of glaucoma or central retinal vein occlusion in the astronauts.

The functional and structural findings in the two mutant mouse models of Hhcy prompted the present study to analyze levels of key enzymes at ages that reflect time points in which only modest GC loss is observed, mild retinal function alteration is detected, and vasculopathy is modest (e.g., 12 and 22 weeks). We were interested in whether there was a compensatory effect of one pathway for the other, for example, that CBS levels are increased in *Mthfr*$^{+/-}$ mutants or MTHFR levels are increased in *Cbs*$^{+/-}$ mutants. We did not observe marked compensatory changes. In *Mthfr*$^{+/-}$ mice, there were no significant changes in MTHFR protein levels despite decreased expression of *Mthfr* RNA at 22 weeks. There was a slight increase in *Cbs* RNA at 12 weeks, which decreased significantly by 22 weeks; there was no change in protein levels. There was an increase in *Cth*

expression initially, but this did not persist, and no changes were observed in CTH protein levels.

In *Cbs*$^{+/-}$ mutant mice, there was no compensatory increase in MTHFR or CTH at the RNA or protein level. There was a marked decrease in *Cbs* RNA expression at 12 and 22 weeks and a dramatic decrease in CBS protein by 22 weeks. This finding was intriguing because, in the transulfuration pathway, there are several factors that are beneficial to retina downstream of CBS including GSH, taurine, and potentially H_2S. We predicted that *Cbs*$^{+/-}$ mutant retinas would have diminished levels of GSH or taurine; however, this was not the case. Total GSH levels and levels of reduced:oxidized GSH in *Cbs*$^{+/-}$ retinas were similar to *Mthfr*$^{+/-}$ and WT mice. A major source of cysteine, the rate-limiting substrate for GSH production, is the cystine-glutamate exchanger, system xc-. As reviewed by McBean,[45] the exchanger is considered the major mechanism for provision of cysteine for GSH, at least in astrocytes, although the transsulfuration pathway can also participate. In the case of the Hhcy models we investigated in this study, it appears that the exchanger is fully functional. Our finding that expression of xCT, the unique component of the exchanger, is robust in *Cbs*$^{+/-}$ and *Mthfr*$^{+/-}$ mice supports this notion. It is not feasible to study the activity of the transporter in the neural retina tissue; however, in future studies we will examine its function in isolated retinal Müller cells under Hhcy conditions. The data suggest that at least through 22 weeks, a decrease in GSH levels does not account for the GC loss and vascular changes observed in the Hhcy models.

We predicted also that because taurine is a downstream product of the transsulfuration pathway that its levels might be altered in *Cbs*$^{+/-}$ retinas. However, our analysis showed very high taurine levels in *Cbs*$^{+/-}$ retinas that were similar to *Mthfr*$^{+/-}$ and WT mice. The transsulfuration pathway is not the sole source of this amino acid in the retina, emphasizing the importance of the Na^+-dependent TAUT in delivery of taurine to retina. Taurine has long been known to be essential for photoreceptor cell survival; however, new studies demonstrate a key role in protecting against retinal GC loss as well.[28] We detected an abundance of TAUT in neural retinas of Hhcy and WT retinas. It may be that taurine in *Cbs*$^{+/-}$ and *Mthfr*$^{+/-}$ retinas is neuroprotective in Hhcy mice, attenuating GC loss. Future studies examining the Hhcy models that lack TAUT would permit this speculation to be tested.

A third important downstream product of the transsulfuration pathway, H_2S, was also evaluated in Hhcy retinas. Hydrogen sulfide levels were markedly elevated in both *Cbs*$^{+/-}$ and *Mthfr*$^{+/-}$ retinas compared with WT. The major enzymes involved in endogenous production of H_2S include CBS and CTH; however, a third enzyme MST can also generate H_2S.[46] We examined levels of MST in *Cbs*$^{+/-}$ and *Mthfr*$^{+/-}$ retinas, but did not observe a statistical difference in protein levels in either mutant mouse model. Thus, MST does not account for the increased level of H_2S in retinas of these mice. The prevailing thought for many years had been that H_2S was a toxic and noxious gas; later, it was considered a metabolic byproduct or a marker of enzymatic activity.[47] Recent studies have ascribed a much more important role to this gaseous molecule. Kimura et al.[48] showed that H_2S facilitates induction of hippocampal long-term potentiation by enhancing activity of *N*-methyl-D-aspartate receptors and might act as a neuromodulator. Indeed, H_2S is now proposed as a novel neurotransmitter, or more accurately a gasotransmitter. Work from Snyder's group suggests that H_2S signals by sulfhydration, which involves modification of cysteine residues on target proteins. There are number of proteins, whose functions are regulated by sulfhydration.[29] It is noteworthy that rather than having a deleterious effect on neurons, H_2S can protect primary cultures of these cells from oxidative toxicity and excitotoxicity. This observation is particularly relevant to retina, in which oxidative stress and excitotoxicity are implicated in disease.

The current findings may help in understanding whether Hhcy is pathogenic or merely a biomarker in certain retinal diseases. Using two mutant models with excess levels of Hcy due to mutations of two arms of the Hcy-methionine metabolic pathway, we were able to interrogate comprehensively levels of several key enzymes and important downstream factors directly relevant to retinal health. We did not observe altered enzyme levels nor marked decreases in GSH or taurine. These data suggest that the neurovascular phenotype may be due to directly to elevated retinal Hcy, which characterizes both models, providing some support for the notion that Hcy is pathogenic and not merely a biomarker for retinal disease. We made an additional observation, however, that was surprising regarding elevated retinal levels of H_2S in the two models. We do not know whether H_2S represents a beneficial phenomenon or whether it is toxic. In other words, would the GC loss and vascular phenotype in the Hhcy mutant mice be worse or better if H_2S was not elevated? There has been one report that elevated H_2S contributes to retinal neovascularization in an ischemia-induced retinopathy; however, the levels of CBS were actually elevated in that model.[39] Future studies will explore the role of elevated H_2S in the Hhcy models, as well various proteins regulated by sulfhydration that may help explain the retinal phenotype observed under Hhcy conditions.

Acknowledgments

The authors thank Rima Rozen, PhD, (McGill University, Montreal, Canada) for providing the founder *Mthfr*$^{+/-}$ mouse breeding pairs to establish our colony.

Supported by National Institutes of Health Grants R01 EY012830 and R01 HL116571.

Disclosure: **X. Cui**, None; **S. Navneet**, None; **J. Wang**, None; **P. Roon**, None; **W. Chen**, None; **M. Xian**, None; **S.B. Smith**, None

References

1. Mudd SH, Skovby F, Levy HL, et al. The natural history of homocystinuria due to cystathionine beta-synthase deficiency. *Am J Hum Genet*. 1985;37:1–31.
2. Hainsworth AH, Yeo NE, Weekman EM, Wilcock DM. Homocysteine, hyperhomocysteinemia and vascular contributions to cognitive impairment and dementia (VCID). *Biochim Biophys Acta*. 2016;1862:1008–1017.
3. Lai WK, Kan MY. Homocysteine-induced endothelial dysfunction. *Ann Nutr Metab*. 2015;67:1–12.
4. Sharma M, Tiwari M, Tiwari RK. Hyperhomocysteinemia: impact on neurodegenerative diseases. *Basic Clin Pharmacol Toxicol*. 2015;117:287–296.
5. Ajith TA, Ranimenon. Homocysteine in ocular diseases. *Clin Chim Acta*. 2015;450:316–321.
6. Huang P, Wang F, Sah BK, et al. Homocysteine and the risk of age-related macular degeneration: a systematic review and meta-analysis. *Sci Rep*. 2015;5:10585.
7. Gopinath B, Flood VM, Rochtchina E, Wang JJ, Mitchell P. Homocysteine, folate, vitamin B-12, and 10-y incidence of age-related macular degeneration. *Am J Clin Nutr*. 2013;98:129–135.
8. Malaguarnera G, Gagliano C, Salomone S, et al. Folate status in type 2 diabetic patients with and without retinopathy. *Clin Ophthalmol*. 2015;9:1437–1442.
9. Srivastav K, Saxena S, Mahdi AA, et al. Increased serum level of homocysteine correlates with retinal nerve fiber layer thinning in diabetic retinopathy. *Mol Vis*. 2016;22:1352–1360.

10. Bulum T, Blaslov K, Duvnjak L. Plasma homocysteine is associated with retinopathy in type 1 diabetic patients in the absence of nephropathy. *Semin Ophthalmol*. 2016;31:198–202.
11. Minniti G, Calevo MG, Giannattasio A, et al. Plasma homocysteine in patients with retinal vein occlusion. *Eur J Ophthalmol*. 2014;24:735–743.
12. Bleich S, Jünemann A, Von Ahsen N, et al. Homocysteine and risk of open-angle glaucoma. *J Neural Transm*. 2002;109: 1499–1504.
13. Vessani RM, Ritch R, Liebmann JM, Jofe M. Plasma homocysteine is elevated in patients with exfoliation syndrome. *Am J Ophthalmol*. 2003;136:41–46.
14. Leibovitzh H, Cohen E, Levi A, et al. Relationship between homocysteine and intraocular pressure in men and women: a population-based study. *Medicine (Baltimore)*. 2016;95:e4858.
15. Pasquale LR, Borrás T, Fingert JH, Wiggs JL, Ritch R. Exfoliation syndrome: assembling the puzzle pieces. *Acta Ophthalmol*. 2016;94:e505–e512.
16. Li J, Xu F, Zeng R, Gong H, Lan Y. Plasma homocysteine, serum folic acid, serum vitamin B12, serum vitamin B6, MTHFR, and risk of normal-tension glaucoma. *J Glaucoma*. 2016;25:e94–e98.
17. Ritch R. Ocular and systemic manifestations of exfoliation syndrome. *J Glaucoma*. 2014;23:S1–S8.
18. Sekeroglu MA, Irkec M, Mocan MC, Orhan M. Hereditary thrombophilic factors in glaucoma. *J Glaucoma*. 2016;25: 203–207.
19. Kang JH, Loomis SJ, Wiggs JL, Willett WC, Pasquale LR. A prospective study of folate, vitamin B_6, and vitamin B_{12} intake in relation to exfoliation glaucoma or suspected exfoliation glaucoma. *JAMA Ophthalmol*. 2014;132:549–559.
20. Ariga M, Nivean M, Utkarsha P. Pseudoexfoliation syndrome. *J Curr Glaucoma Pract*. 2013;7:1118–1120.
21. Ganapathy PS, Moister B, Roon P. Endogenous elevation of homocysteine induces retinal neuron death in the cystathionine-beta-synthase mutant mouse. *Invest Ophthalmol Vis Sci*. 2009;50:4460–4470.
22. Lawrance AK, Racine J, Deng L, Wang X, Lachapelle P, Rozen R. Complete deficiency of methylenetetrahydrofolate reductase in mice is associated with impaired retinal function and variable mortality, hematological profiles, and reproductive outcomes. *J Inherit Metab Dis*. 2011;34:147–157.
23. Yu M, Sturgill-Short G, Ganapathy P, Tawfik A, Peachey NS, Smith SB. Age-related changes in visual function in cystathionine-beta-synthase mutant mice, a model of hyperhomocysteinemia. *Exp Eye Res*. 2012;96:124–131.
24. Tawfik A, Markand S, Al-Shabrawey M, et al. Alterations of retinal vasculature in cystathionine-β-synthase heterozygous mice: a model of mild to moderate hyperhomocysteinemia. *Am J Pathol*. 2014;184:2573–2585.
25. Markand S, Saul A, Roon P, et al. Retinal ganglion cell loss and mild vasculopathy in methylene tetrahydrofolate reductase (Mthfr)-deficient mice: a model of mild hyperhomocysteinemia. *Invest Ophthalmol Vis Sci*. 2015;56:2684–2695.
26. Dun Y, Thangaraju M, Prasad P, Ganapathy V, Smith SB. Prevention of excitotoxicity in primary retinal ganglion cells by (+)-pentazocine, a sigma receptor-1 specific ligand. *Invest Ophthalmol Vis Sci*. 2007;48:4785–4794.
27. Rathbun WB. Glutathione in ocular tissues. In: Dolphin D, Avramovic O, Poulson R, editors. *Glutathione: Chemical, Biochemical, and Medical Aspects*. New York: Wiley; 1989: 469–510.
28. Froger N, Moutsimilli L, Cadetti L, et al. Taurine: the comeback of a neutraceutical in the prevention of retinal degenerations. *Prog Retin Eye Res*. 2014;41:44–63.
29. Paul BD, Snyder SH. H_2S: a novel gasotransmitter that signals by sulfhydration. *Trends Biochem Sci*. 2015;40:687–700.
30. Chang B, Hurd R, Wang J, Nishina P. Survey of common eye diseases in laboratory mouse strains. *Invest Ophthalmol Vis Sci*. 2013;54:4974–4781.
31. Wang J, Saul A, Roon P, Smith SB. Activation of the molecular chaperone, sigma 1 receptor, preserves cone function in a murine model of inherited retinal degeneration. *Proc Natl Acad Sci U S A*. 2016;113:E3764–E3472.
32. Wang J, Shanmugam A, Markand S, Zorrilla E, Ganapathy V, Smith SB. Sigma 1 receptor regulates the oxidative stress response in primary retinal Müller glial cells via NRF2 signaling and system xc(-), the Na(+)-independent glutamate-cystine exchanger. *Free Radic Biol Med*. 2015;86:25–36.
33. Dun Y, Mysona B, Van Ells T, et al. Expression of the cystine-glutamate exchanger (xc-) in retinal ganglion cells and regulation by nitric oxide and oxidative stress. *Cell Tissue Res*. 2006;324:189–202.
34. Zhang L, Meng WQ, Lu L, et al. Selective detection of endogenous H_2S in living cells and the mouse hippocampus using a ratiometric fluorescent probe. *Sci Rep*. 2014;4:5870.
35. Peng B, Chen W, Liu C, et al. Fluorescent probes based on nucleophilic substitution-cyclization for hydrogen sulfide detection and bioimaging. *Chemistry*. 2014;20:1010–1016.
36. Lewerenz J, Hewett SJ, Huang Y, et al. The cystine/glutamate antiporter system x(c)(-) in health and disease: from molecular mechanisms to novel therapeutic opportunities. *Antioxid Redox Signal*. 2013;18:522–555.
37. Sato H, Tamba M, Ishii T, Bannai S. Cloning and expression of a plasma membrane cystine/glutamate exchange transporter composed of two distinct proteins. *J Biol Chem*. 1999;274: 11455–11458.
38. El-Sherbeny A, Naggar H, Miyauchi S, et al. Osmoregulation of taurine transporter function and expression in retinal pigment epithelial, ganglion, and Müller cells. *Invest Ophthalmol Vis Sci*. 2004;45:694–701.
39. Gersztenkorn D, Coletta C, Zhu S, et al. Hydrogen sulfide contributes to retinal neovascularization in ischemia-induced retinopathy. *Invest Ophthalmol Vis Sci*. 2016;57:3002–3009.
40. Dun Y, Thangaraju M, Prasad P, Ganapathy V, Smith SB. Prevention of excitotoxicity in primary retinal ganglion cells by (+)-pentazocine, a sigma receptor-1 specific ligand. *Invest Ophthalmol Vis Sci*. 2007;48:4785–4794.
41. Moore P, El-sherbeny A, Roon P, Schoenlein PV, Ganapathy V, Smith SB. Apoptotic cell death in the mouse retinal ganglion cell layer is induced in vivo by the excitatory amino acid homocysteine. *Exp Eye Res*. 2001;73:45–57.
42. Chang HH, Lin DP, Chen YS, et al. Intravitreal homocysteine-thiolactone injection leads to the degeneration of multiple retinal cells, including photoreceptors. *Mol Vis*. 2011;17: 1946–1956.
43. Ganapathy PS, Perry RL, Tawfik A, et al. Homocysteine-mediated modulation of mitochondrial dynamics in retinal ganglion cells. *Invest Ophthalmol Vis Sci*. 2011;52:5551–5558.
44. Zwart SR, Gibson CR, Mader TH, et al. Vision changes after spaceflight are related to alterations in folate- and vitamin B-12-dependent one-carbon metabolism. *J Nutr*. 2012;142:427–431.
45. McBean GJ. The transsulfuration pathway: a source of cysteine for glutathione in astrocytes. *Amino Acids*. 2012; 42:199–205.
46. Kimura Y, Goto Y, Kimura H. Hydrogen sulfide increases glutathione production and suppresses oxidative stress in mitochondria. *Antioxid Redox Signal*. 2010;12:1–13.
47. Kimura H. Hydrogen sulfide and polysulfides as signaling molecules. *Proc Jpn Acad Ser B Phys Biol Sci*. 2015;91:131–159.
48. Abe K, Kimura H. The possible role of hydrogen sulfide as an endogenous neuromodulator. *J Neurosci*. 1996;16:1066–1071.

Investigative Ophthalmology & Visual Science